An efficient approach for predicting low-velocity impact force and damage in composite laminates

Zhang, J. and Zhang, X.

Zhang, J, Zhang, X, An efficient approach for predicting low-velocity impact force and damage in composite laminates, Composite Structures (2015), doi: http://dx.doi.org/10.1016/j.compstruct. 2015.04.023

An efficient approach for predicting low-velocity impact force and damage in composite laminates

Jikui Zhang[a], Xiang Zhang[1b]

[a] Department of Aircraft Design, Beihang University, Beijing 100191, PR China
[b] Faculty of Engineering and Computing, Coventry University, Coventry CV1 2JH, UK

Abstract

An efficient approach is presented to predict the critical impact force and corresponding damage in composite laminates subjected to low-velocity impact. In developing such approach, stress analysis was conducted first for a 4 mm thick quasi-isotropic laminate to determine the potential failure modes and locations under the critical impact force. Three finite element models were subsequently built to simulate the damage in the upper, middle and lower interfaces and investigate the effect of each damage mode on the laminate stiffness. It is found that delamination adjacent to the impact point is suppressed by the high compressive through-thickness stress resulting in negligible reduction of the laminate stiffness. Both the delamination in interfaces adjacent to the mid-thickness plane and matrix fracture on the lower face can cause the first load drop, which corresponds to the critical impact force. The former is the main causative mechanism for the laminate studied in this paper. A simplified and efficient finite element model, which takes account of the delamination damage adjacent to the mid-thickness plane and the lower face, is developed that is computationally affordable and delivers acceptable prediction of the critical impact force, damage shape and size, by both quasi-static load and dynamic impact analyses.

Keywords: low-velocity impact; finite element; delamination; cohesive zone model; critical impact force

1. Introduction

Advanced carbon fibre reinforced plastics (CFRP) have been increasingly used in the airframe primary structures due to their excellent mechanical properties and low specific weight. However poor properties in the through-thickness direction make CFRP particularly susceptible to the low velocity impact. Composite laminates exhibit a relatively brittle behaviour and can undergo internal damage in forms of matrix cracks, fibre breakage and delamination when they are subjected to foreign object impacts. These damages (in particular delamination) may propagate undetected during the service resulting in unexpected failure of the component, especially for the primary structures loaded in compression. Therefore, it is essential to develop a computer-based design tool to predict the damage onset and evolution in composite structures under impact.

The cohesive zone model (CZM), which combines strength-based criteria with fracture mechanics energy criteria, has attracted considerable interests in recent years. Cohesive elements placed at the interface between layers have been successfully used in various studies to model the delamination induced by low velocity impact in composite laminates with cross-ply [1-3] and clustered layers [4-6]. Several CZMs have achieved acceptable prediction for simulating the impact damage initiation

[1] Corresponding author. Tel.: +44 24 77658599, E-mail address: xiang.zhang@coventry.ac.uk (X. Zhang); zjk@buaa.edu.cn (J. Zhang)

and propagation in multi-direction composites [7-9], e.g. $[0_3/+45/45]_S$, $[0_2/45_2/90_2/-45_2]_S$, and $[45/-45/90/0]_S$ laminates. However, these laminates consisted of fewer than 7 interfaces that need to be modelled by cohesive elements. Lopes et al [10] developed a finite element (FE) model to simulate the damage of a 24 ply laminate $[\pm45/90/0/45/0_4/-45/0_2]_S$ under low-velocity impact. Cohesive elements were inserted in each interface to simulate the delamination initiation and propagation. It took 4 to 5 days to complete a simulation using a cluster 32 CPU's workstation. Therefore, it is not yet possible to use the CZM as a design tool for realistic structures.

As pointed out in the open literature [11-15], there are two different phases in the impact response during the damage process. First, the impact force reaches a threshold value, also defined as the critical force that results from the delamination onset causing a sudden loss of the laminate stiffness and drop of the impact force in the response. Second, the damage size increases with the force until the force reaches its maximum, defined as the peak force. The difficulty to predict the peak force of thick multi-direction laminates under impact loading is mainly due to the complexity of the physical phenomena involved during the damage propagation, which require accurate modelling of the dynamics response, contact formulation, interlaminar friction, interaction of various failure modes, including matrix cracking, delamination and fibre breakage. Current computer models will take days to simulate a simple test coupon, which are not yet regarded as design tools. However, it is feasible to develop an efficient FE model to predict the critical impact force that is also defined as the Delamination Threshold Load (DTL) [13, 16-17], which is a measurement of the damage resistance of a composite material [18]. The critical force can be related to critical impact energy for design purpose. Extensive experimental tests have shown that the critical force is independent of the specimen size, boundary condition and impact energy [12, 16, 18-19]. Therefore, it can aid the design process by relating the coupon test data with realistic structural elements as long as the thickness and the stacking sequence are the same.

The prediction of critical impact force has been attempted by many researchers. Sjoblom [20] predicted that the critical damage initiation load is related to $t^{3/2}$, where t is the laminate thickness. Davies et al. [21-22] developed an equation based on the mode II fracture to determine the onset of the delamination based on the simple beam theory and assumption of quasi-isotropic property with one delamination in the mid thickness. This equation also indicates that the critical force is proportional to $t^{3/2}$, which has been supported by a number of tests [23-25] and provides an estimate of the critical force for a given quasi-isotropic laminate. Independent experiment by Olsson [26] also shows the correlation of critical force with $t^{3/2}$.

To summarise, critical impact force is a key parameter to characterise the damage resistance of composite materials. Although the equation developed by Davies et al. [21-22] gives acceptable results for quasi-isotropic laminates, it cannot be applied to more complex laminates or realistic structures, e.g. non-quasi-isotropic layups, multiple delamination and delamination that is triggered by early matrix cracking (bending mode dominated thin or larger plate or weaker resin properties). Therefore, an FE-based design tool is still needed to predict the critical impact force of realistic structures.

The aim of the work presented in this paper is to develop an efficient approach for predicting the critical impact force under low velocity impact. First, three FE models have been developed to simulate the damage located in the top and middle interfaces, and also the laminate's back face, and

their effects on the stiffness degradation. Second, based on these models, a computationally efficient model is established and the prediction results are compared with the experimental tests in terms of the critical force, force-displacement relation, and damage shape and size.

2. Strategy of modelling approach

In this paper, a previously conducted low velocity impact test [19, 27] is modelled. The material is unidirectional pre-preg IM7/977-3. Ply mechanical properties obtained from [19, 27] are given in Table 1, where E_{xx}, E_{yy} and E_{zz} are respectively the Young's modulus of the fibre, transverse to the fibre and normal directions, G_{xy}, G_{xz} and G_{yz} the shear moduli, v_{xy}, v_{xz} and v_{yz} the Poisson's ratios. The interface stiffness values in the normal and two shear directions, K_n, K_s, and K_t, are derived and shown in Table 1.

Table 1 Mechanical properties of IM7/977-3 laminate [27]

Lamina ply	Cohesive interface
Elastic modulus (GPa)	Stiffness (GPa/m)
E_{xx}=162, E_{yy}= E_{zz}=8.34, G_{xy}= G_{xz}= G_{yz}=4.96	K_N=240000, K_s= K_t=86000
Poisson's ratio v_{xy}=v_{xz}=v_{yz}=0.27	Normal strength N=64 MPa
Longitude tension and compression strength (MPa)	Shear strength S=T=121 MPa
X_T=2275, X_C=1680	Critical strain energy release rate **(**J/m^2**)**
Transverse tension and compression strength (MPa)	G_{IC} = 320 G_{IIC} = G_{IIIC}=580
Y_T=64, Y_C=186	
Shear strength (MPa) S_{xy}=121, S_{xz}=S_{yz}=127	

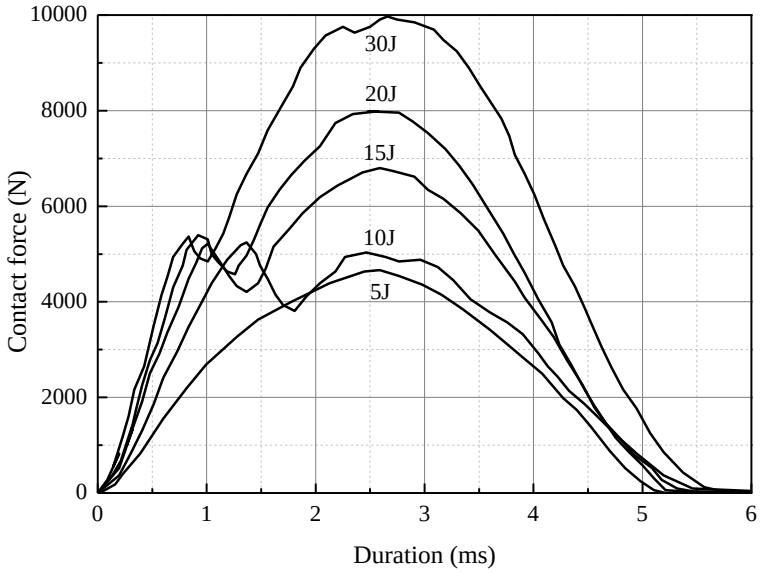

Fig. 1 Filtered impact force vs. time history of low velocity impact test [19, 27] (test specimen size 150×100 mm; inside the support fixture 125×75 mm)

Standard test coupons are of 150×100 mm nominal size with quasi isotropic stacking sequence $[-45/0/45/90]_{4S}$, with a nominal ply thickness of 0.125 mm, 32 plies resulted in a panel of 4 mm nominal thickness. Impact test was conducted using a Rosand instrumented falling weight Type 5 impact tester comprising a load cell detecting the force applied to the impact target. The diameter of the hemispherical impactor was 15.75 mm. The impact support fixture was a 20 mm thick steel plate

with a 125×75 mm cut out. Four clamps were used to restrain the test coupon during the impact. Coupons were impacted at 5, 10, 15, 20 and 30 J. Filtered impact force vs. time history of five individual tests is shown in Fig. 1. A critical impact force of about 5400 N can be clearly observed, that is the first load drop point. Following the impact test, the damage extent in the test coupons was measured using an immersion ultrasound scanner (C-scan).

Although several different failure modes can occur under the low velocity impact load, major efforts have been focused on the modelling of delamination. The CZM, which places the cohesive elements in the interfaces of laminate to calculate the interlaminar cohesive forces, is the most common approach used in the literature. However, it should be pointed out that the CZM relies on predefined interfaces that constrain the interlaminar crack paths. When the crack path is unknown, cohesive elements must be placed in all the interfaces of the laminate layers, which is computationally expensive for the thick and multi-direction laminates.

To reduce the number of interfaces where the cohesive elements need to be defined, stress analysis was conducted first to determine the potential failure modes and location under the critical force. As shown in Fig. 2a, the laminate is modelled by continuum solid element (designated as C3D8R in ABAQUS). The smallest element size in the impact zone is 0.44 × 0.44 mm. Each element layer represents one lamina ply. The zero-thickness cohesive elements (COH3D8) are inserted in all the interfaces. The reason to have the cohesive elements in the stress analysis model is to facilitate a direct comparison with the fracture analysis models presented in Section 3. Figure 2b shows a fracture analysis model where the cohesive element zone is reduced to 50 x 50 mm to model the delamination under the impactor. The impactor is modelled as a rigid body due to the relatively smaller deformation of the impactor compared with that of the laminate. The interaction between the plate and impactor is simulated by surface-to-surface contact pairs. A total of 112000 solid elements and 105000 cohesive elements are used in the FE model to calculate the stress distribution of the impacted laminate. It is assumed that no damage will occur in the solid and cohesive elements.

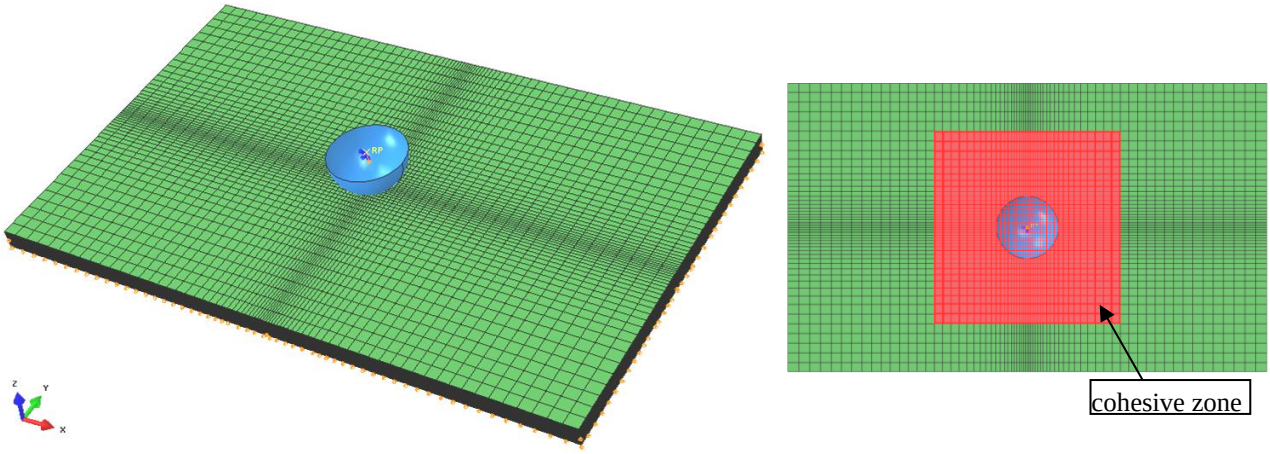

(a) (b)

Fig. 2 Three dimensional FE models: (a) stress analysis model (model size 125×75 mm, cohesive zone 125×75 mm), (b) fracture analysis model in Sections 3 and 4 (cohesive zone: 50×50 mm)

To save the computation time, quasi-static load is applied to simulate the low-velocity impact event. A displacement in the *z*-direction is applied to the impactor instead of the impactor mass and velocity. The similarity of quasi-static load and low-velocity impact in terms of the contact force and damage

area has been reported in [19, 28-29], which demonstrates that the relation of the impact force and displacement is not changed by the impact velocity in the low velocity range, because the influence of inertia caused by the dynamic load is very small and thus can be neglected within the low velocity range [30].

According to the experimental result [19], the displacement of the impactor is about 2 mm at the critical force of 5400N. This displacement is applied to the impactor under the displacement controlled loading model. The distributions of normal stress (σ_{zz}), interlaminar shear stress (τ_{xz}) and in-plane transverse stress (σ_{yy}) are shown in Fig. 3 and 4. There are three likely mechanisms for delamination onset and propagation as explained in the following.

(1) Delamination due to the high interlaminar shear stress τ_{xz} adjacent to the impact point. However, the compressive through-thickness stress (σ_{zz}) is also very high in this local area, such as in the interfaces 1, 5, 9 and 13, as shown in Fig. 4a and b. In this area, the combined effect of τ_{xz} and σ_{zz} should be taken into account since compressive σ_{zz} is likely to suppress the delamination onset and propagation by introducing interlaminar friction.

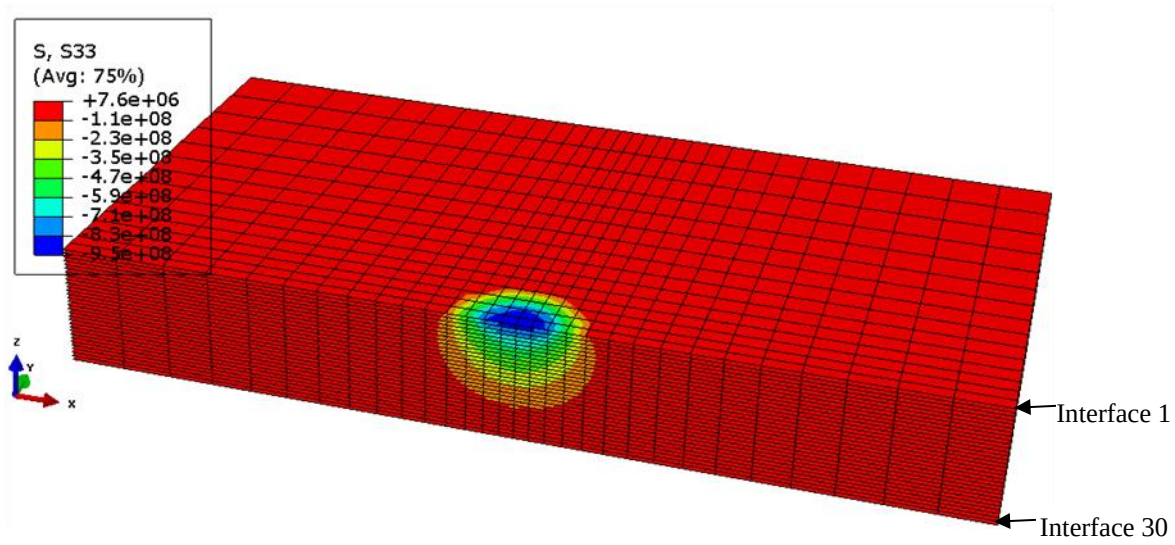

(a)

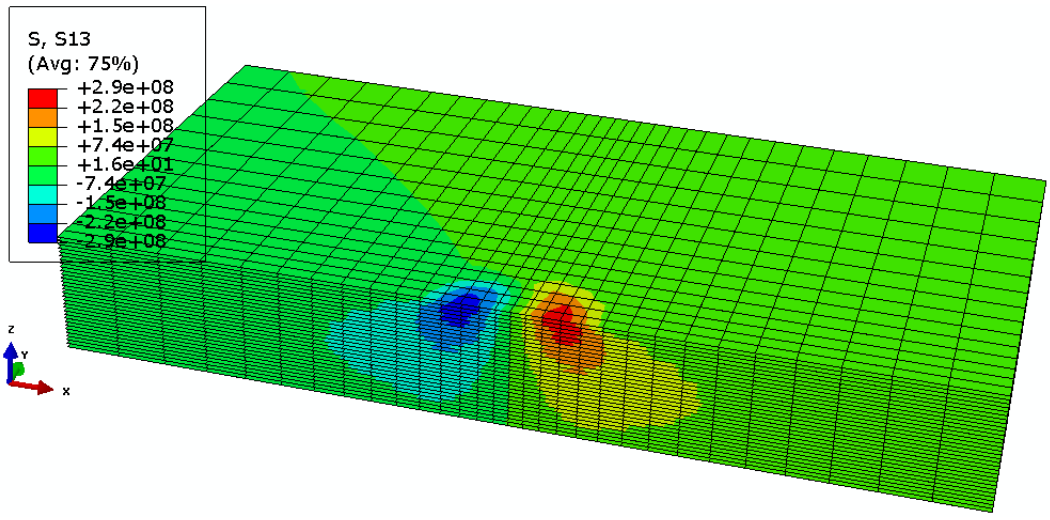

(b)

Fig. 3 (a) Normal σ_{zz} and (b) shear stress τ_{xz} distribution in the cohesive interface elements (unit: Pa)

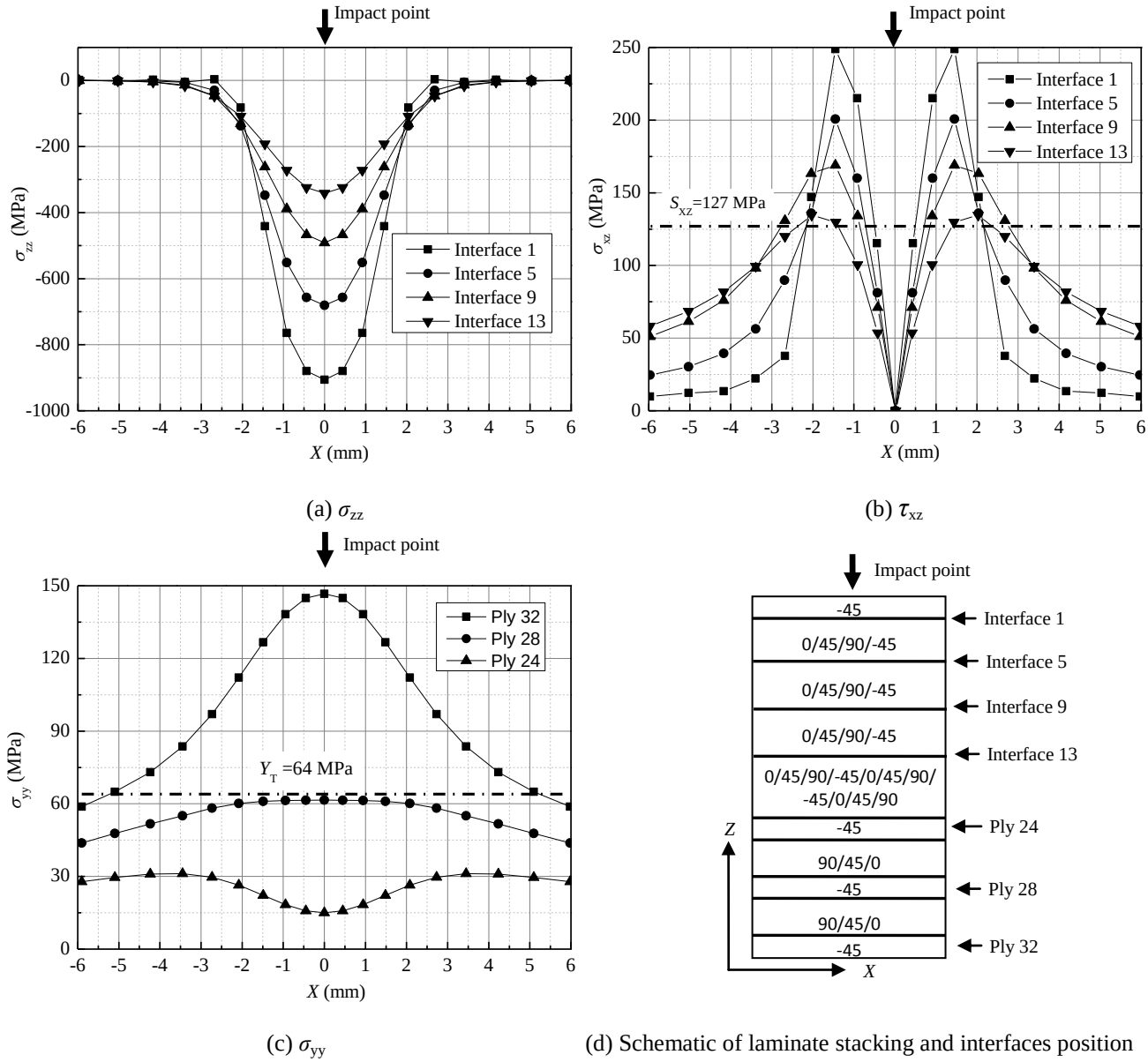

Fig. 4 Stress distributions in the laminate under the critical impact force (QSL stress analysis model Fig. 2a)

(2) Delamination due to the interlaminar shear stresses (τ_{xz}) adjacent to the mid-thickness plane. As shown in Fig. 4a and b, in the area of interfaces 9 and 13 at 2 mm away from the impact point, σ_{zz} is much lower and its effect on delamination suppression could be neglected. Meanwhile, τ_{xz} is higher than the shear strength (S_{xz}); hence it could cause the interlaminar delamination. Therefore, in this study, the CZM is adopted for the interfaces from 9 to 22.

(3) Delamination due to the matrix cracking caused by the tensile bending stress (σ_{yy}) on the lower surface, such as ply 32 and 28 shown in Fig. 4c. These cracks act as a stress-raiser which precipitates delamination in the adjacent layer. This effect is restricted to the back face plies for σ_{yy} is reduced rapidly along the thickness direction. For example in this study, the in-plane transverse stress (σ_{yy}) in ply 24 is much lower than the transverse strength (Y_T), as shown in Fig. 4c.

On the basis of the stress analysis, three finite element models are developed to simulate the damage in the upper and middle interfaces and the lower surface separately, see details in Section 3. The

effect of each damage mode on the global stiffness is investigated. To establish a computationally affordable model, only those interfaces, where damage has considerably degraded the laminate stiffness, will be modelled by the cohesive elements.

3. Development of computationally affordable models

3.1 Damage modelling

The impact load history provides important information on the damage onset and propagation. The first load drop does not physically represent the initiation of damage as the sub-critical matrix cracks and small delamination may initiate at lower force [11]. Actually, it represents the initial force value, at which a significant change in the laminate stiffness properties can be detected [16]. It corresponds to the occurrence of damage in terms of matrix cracking, fibre breakage and delamination. These damages are classically grouped into the in-plane and interlaminar damage, which are modelled in this paper by different approaches.

(1) In-plane damage. If the impact energy is sufficiently high, it may result in significant in-plane damage in terms of fibre breakage and matrix cracking. It is necessary to degrade the structural stiffness matrix in models when significant in-plane damage occurs in order to predict the impact force correctly. The 3D Hashin-type failure criterion and material property degradation rules used in [31] are adopted to model the matrix cracking in tension and compression, fibre failure in tension and compression, and fibre-matrix shear out, as summarised in Table 2, where σ_{xx} and σ_{yy} are the in-plane stresses in the fibre and transverse directions, τ_{xy} and τ_{yz} the shear stresses, X_T and X_C the fibre tension and compression strength, Y_T and Y_C the matrix tension and compression strength, S_{xy} and S_{yz} the shear strength. Subscript "d" denotes degraded material properties. A user defined subroutine (designated as USDFLD in ABAQUS) is developed for implementing the Hashin failure criterion in Table 2.

Table 2 In-plane 3D Hashin-type failure criteria and material property degradation rules [31]

Failure Mode	Failure criterion	Material property degradation rule
Matrix tension cracking	$\left(\frac{\sigma_{yy}}{Y_T}\right)^2+\left(\frac{\tau_{xy}}{S_{xy}}\right)^2+\left(\frac{\tau_{yz}}{S_{yz}}\right)^2\geq 1$	$E_{yy,d}=0.2E_{yy}\quad G_{xy,d}=0.2G_{xy}\quad G_{yz,d}=0.2G_{yz}$
Matrix compression cracking	$\left(\frac{\sigma_{yy}}{Y_C}\right)^2+\left(\frac{\tau_{xy}}{S_{xy}}\right)^2+\left(\frac{\tau_{yz}}{S_{yz}}\right)^2\geq 1$	$E_{yy,d}=0.4E_{yy}\quad G_{xy,d}=0.4G_{xy}\quad G_{yz,d}=0.4G_{yz}$
Fibre tension failure	$\left(\frac{\sigma_{xx}}{X_T}\right)^2+\left(\frac{\tau_{xy}}{S_{xy}}\right)^2+\left(\frac{\tau_{yz}}{S_{yz}}\right)^2\geq 1$	$E_{xx,d}=0.07E_{xx}$
Fibre compression failure	$\left(\frac{\sigma_{xx}}{X_C}\right)^2\geq 1$	$E_{xx,d}=0.14E_{xx}$
Fibre-matrix shear-out	$\left(\frac{\sigma_{xx}}{X_C}\right)^2+\left(\frac{\sigma_{xy}}{S_{xy}}\right)^2+\left(\frac{\sigma_{yz}}{S_{yz}}\right)^2\geq 1$	$G_{xy,d}=\upsilon_{xy,d}=0$

(2) Interlaminar damage. CZM has been employed by many researchers [1-9] to simulate the delamination growth in composite laminates. The failure of cohesive element is based on the interactive mixed mode criteria for both the initiation and propagation of the delamination. The model works well if the through-thickness stress is in tension or relatively low in compression. In this study, cohesive elements are used to the interfaces that are far away form the impact point. A stress-based quadratic traction-serpration law is used to detect the delamination initiation:

$$\left(\frac{t_{\mathrm{n}}}{N}\right)^2+\left(\frac{t_{\mathrm{s}}}{S}\right)^2+\left(\frac{t_{t}}{T}\right)^2\geq 1 \tag{1}$$

where t_{n}, t_{s}, and t_{t} are the interface stresses in the normal and two shear directions, respectively, and N, S and T the corresponding interface strength. Delamination propagation under the mixed-mode loading is modelled by the following interactive criterion:

$$\left(\frac{G_{\mathrm{I}}}{G_{\mathrm{IC}}}\right)+\left(\frac{G_{\mathrm{II}}}{G_{\mathrm{IIC}}}\right)+\left(\frac{G_{\mathrm{III}}}{G_{\mathrm{IIIC}}}\right)\geq 1 \tag{2}$$

where G_{I}, G_{II} and G_{III} are the strain energy release rates under the mode I, II and III respectively, G_{IC}, G_{IIC} and G_{IIIC} the critical strain energy release rates.

For the upper interfaces close to the impact point, normal stress (σ_{zz}) is considerable high in compression that greatly increases the interlaminar shear strength. In this paper, a surface-based cohesive contact model available in ABAQUS is adopted to model the combined effect of τ_{xz} and σ_{zz}. Surface-based cohesive contact [32] allows specification of generalised traction-separation behaviour for two adjacent surfaces. This behaviour offers capability of modelling failure that is very similar to the cohesive element approach that is defined using a traction-separation law. However, the surface-based cohesive model is much easier to define and allows simulation of a wider range of cohesive interactions, such as interlaminar delamination and contact phenomenon of laminates subjected to impact load [30]. Failure criteria of interface used in surface-based cohesive contact model is the same as that used in the cohesive element model, as given in eqs. (1) and (2). It is implemented in the ABAQUS code without the need of defining any special elements or user specific code.

3.2 Finite element models to identify crucial damage modes

As mentioned above, it is computationally expensive if one model has all potential damage modes. Based on the stress analysis in Section 2 and bearing in mind of the aim to predict the critical impact force and the corresponding damage, three finite element models are developed to simulate the impact damage in the upper and middle interfaces and lower face separately, as shown in Fig. 5. The cohesive zone size in the models is 50×50 mm, as shown in Fig. 2b. A *z*-direction displacement of 2.5 mm is applied to the impactor in order to capture the critical impact force.

Model 1 (Fig. 5a) focuses on the delamination adjacent to the impact point, i.e. the upper interface. Surface based contact model is adopted for the interfaces of 1-8 in order to model the effect of compressive σ_{zz} on the delamination onset and propagation. Matrix cracking and fibre breaking are also modelled in plies 1-9 owing to the high compressive in-plane stress (σ_{xx} and σ_{yy}) caused by the bending effect.

Model 2 (Fig. 5b) mimics the internal delamination due to the high interlaminar shear stresses in the interfaces near the mid-thickness region. Cohesive elements are inserted at interface 9-22 to model the mode II delamination onset and propagation. No interface element is inserted to the mid thickness plane interface between the 90/90 plies, since no delamination is expected between the same fibre orientation plies.

Model 3 (Fig. 5c) concentrates on the damage evolution on the lower face due to the tensile bending stress. Matrix cracking and fibre breaking are modelled in the 25-32th plies. Cohesive elements are inserted for the 23-30th interfaces to model the delamination caused by the matrix cracks.

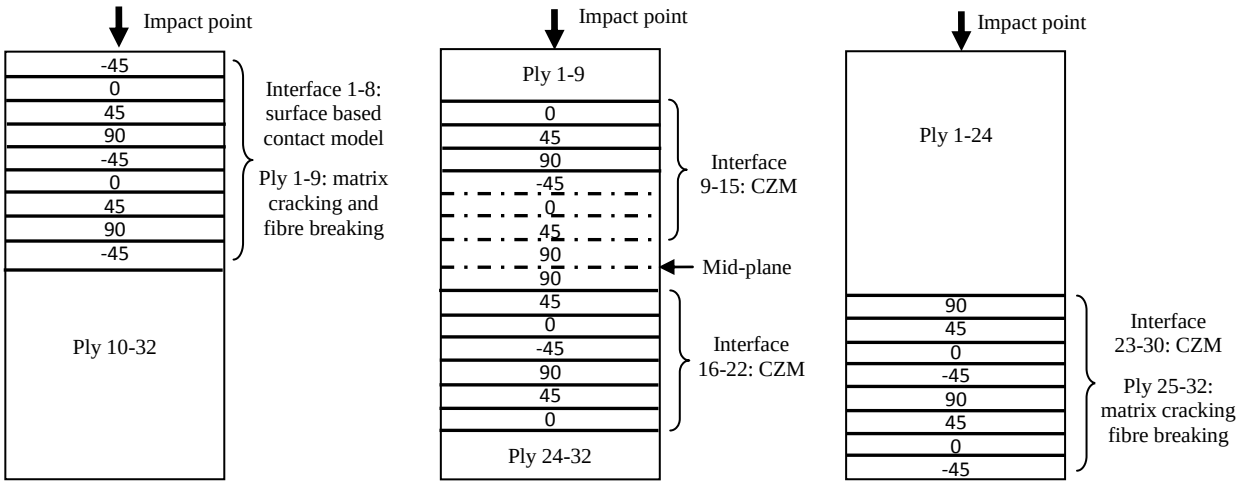

(a) Model 1 (b) Model 2 (c) Model 3

Fig. 5 Schematics of damage and interface definition for finite element models in this study

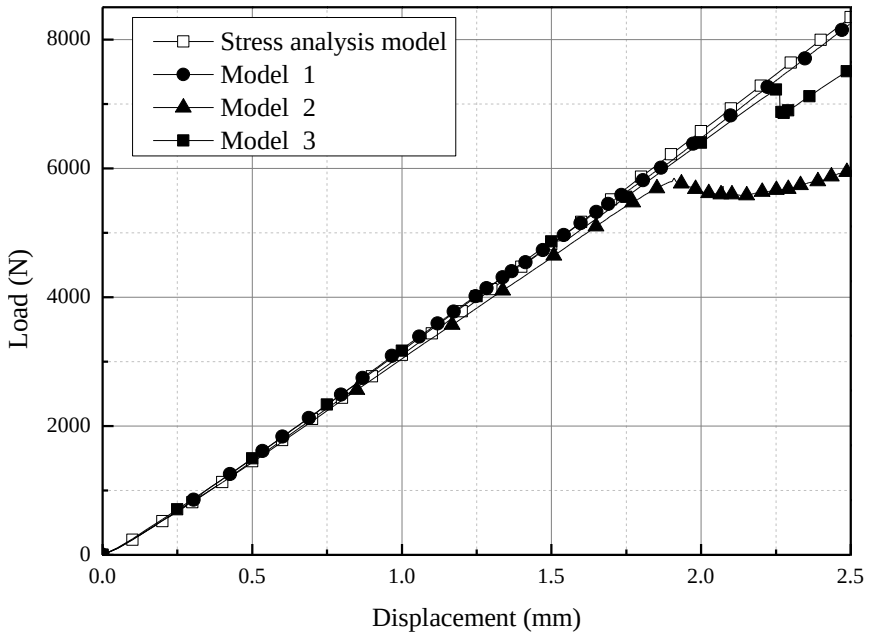

Fig. 6 Comparison of calculated impactor contact force vs. displacement

Fig. 6 shows calculated contact force vs. displacement relation using the three models and comparison with that from the stress analysis model presented in Section 2 that does not model any damage. Following observations are made.

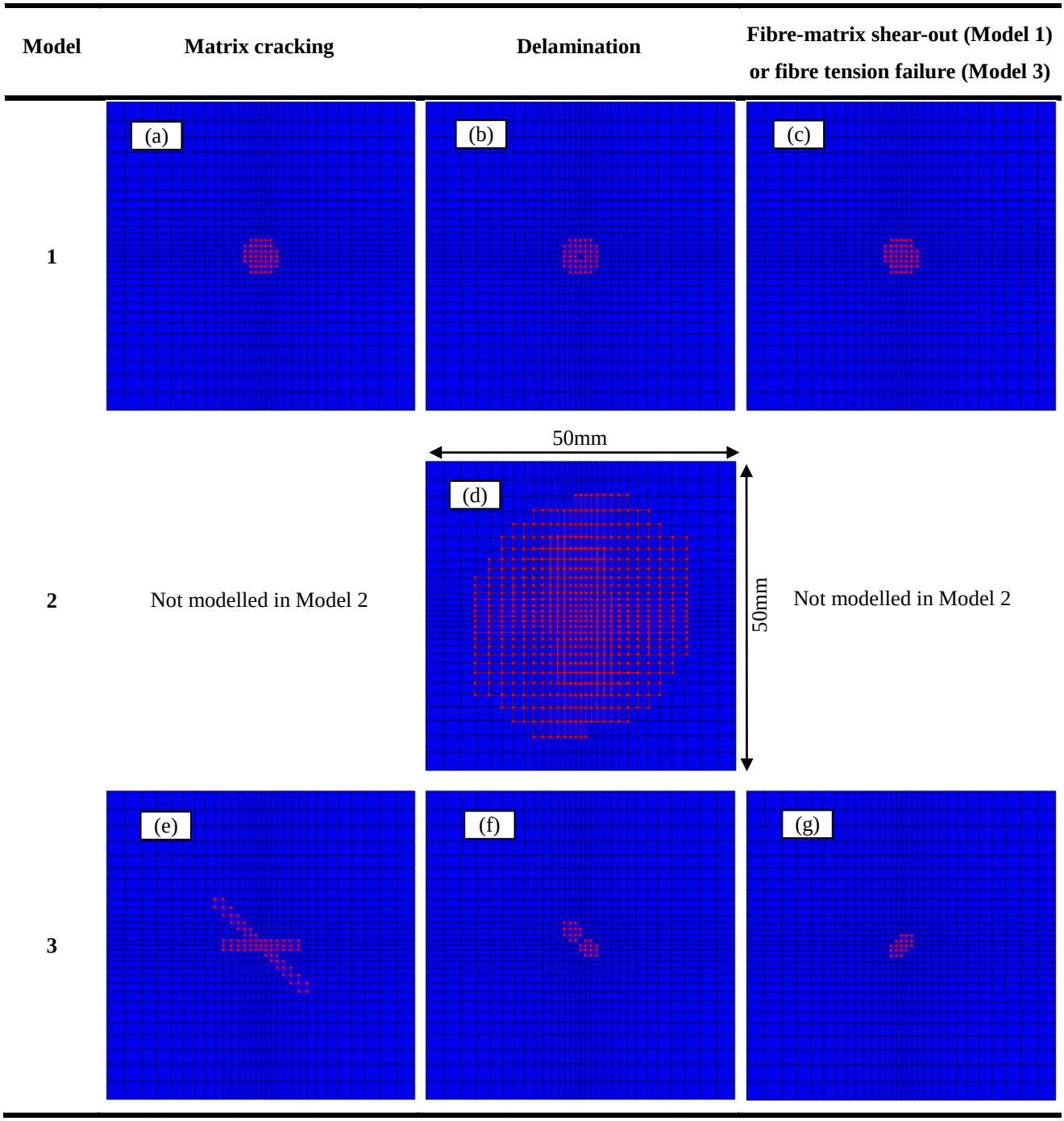

Fig. 7 Predicted damage areas by Models 1, 2 and 3 (showing the sum of damage at different depths)

Calculated contact force vs. displacement by Model 1 almost coincides with the stress analysis model, indicating the delamination onset and propagation at the upper interfaces are inhibited by the high compressive through-thickness stress, as shown in Fig. 7b. Only a few of elements adjacent to the impact point are detected with matrix cracking and fibre-matrix shear-out, as shown in Fig. 7a and 7c. Fibre compression failure does not occur in this model. These damage modes slightly affect the laminate overall stiffness, but can be neglected reasonably for saving the computational time.

Calculated first load-drop point by Model 2 is about 5800N and the corresponding displacement is 1.9mm, which is close to the experimental critical force 5400N as shown in Fig. 1. Delamination predicted by Model 2 is shown in Fig. 7d, which is much large than those predicted by Model 1 (Fig.

7b) and Model 3 (Fig. 7f), implying that internal delamination adjacent to the mid plane is the main cause for the first load drop of the laminate studied in this paper.

The slope of calculated contact force vs. displacement by Model 3 is smaller than that predicted by the stress analysis model due to the extensive matrix cracking. However, the effect of matrix crack and induced delamination on the laminate stiffness is much smaller than the effect of the delamination near the mid-thickness interfaces of Model 2. It should be pointed out that there is also a load drop at about 7720 N in Model 3, which is much higher than the measured critical force 5400 N. This could be explained by the lack of mid-thickness delamination in Model 3, in which only the back-face fibre breakage due to the bending induced tension stress is modelled (Fig. 7g).

4. Results and discussion

4.1 A new efficient FE model for predicting critical impact force

Based on the analyses presented in Section 3, a simplified finite element model (Model 4) is established to predict the critical force of thick multi-direction laminate, as shown in Fig. 8a. Cohesive elements are inserted in interfaces 9-22 adjacent to the mid thickness since the delamination in these interfaces is the main cause for the first load drop. Cohesive elements are also inserted in interfaces 27-30 to capture the delamination induced by the back face matrix cracking. Damage in interfaces 1-8 are not modelled, since it only slightly affects the stiffness of the impacted laminate.

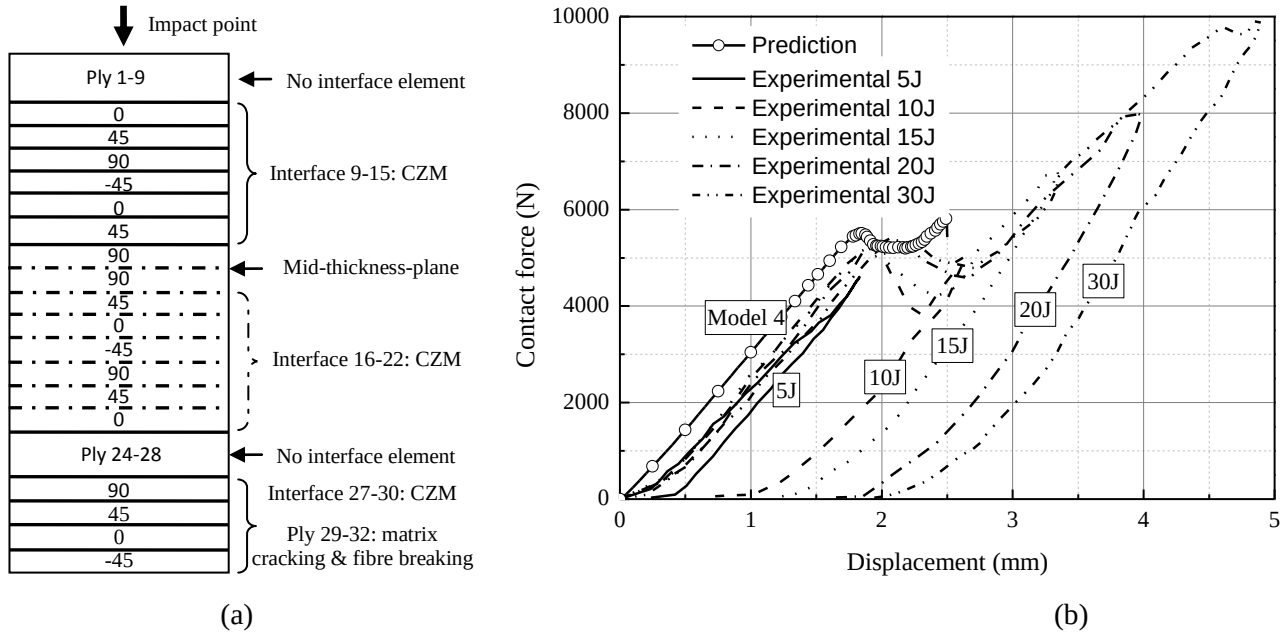

Fig. 8 (a) Schematic of Model 4, (b) predicted contact force vs. displacement by Model 4

Fig. 8b shows the comparison of contact force vs. displacement between the experimental and prediction by Model 4. The slope of the predicted agrees well with the experimental measurement. Calculated first load drop is 5510 N, which is very close to the experimental critical force 5400 N. Predicted delamiantion area is compared with the ultrasound measurement of the 10J impact, since the critical force almost equals to the maximum force for this test (Fig. 1). As shown in Fig. 9, the shape of predicted delamination is similar to the test result. Both the predicted damage width and length are smaller than those of the test result. It could be explained that in the experiment further damage propagation might have ocurred beyond the critical force.

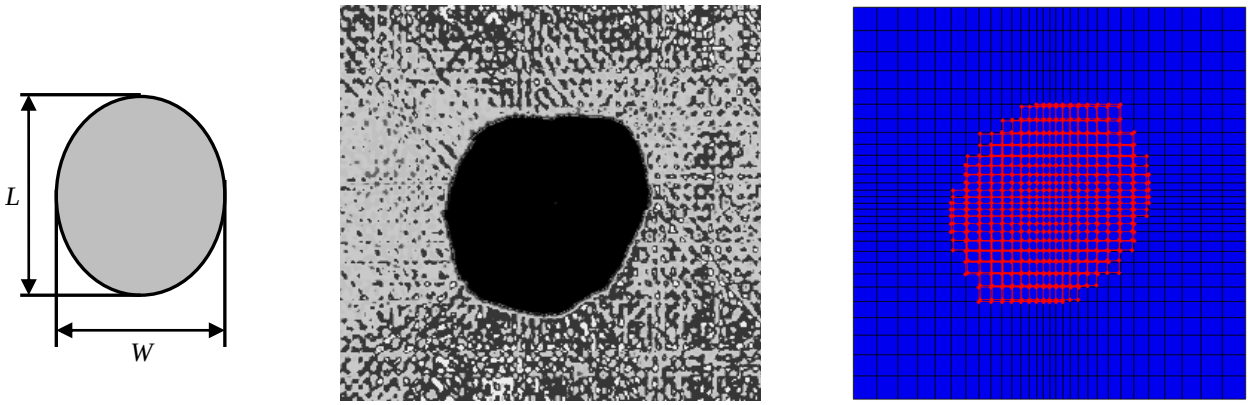

(a) W=29.08 L=31.09 (b) W=23.52 L=25.74

Fig. 9 Comparison of damage shape and size: (a) ultrasound C-scan of 10J impacted laminate, (b) QSL model predicted damage areas corresponding to critical impact force (showing the sum of damage at different depths, unit: mm)

In this paper, all the analyses are carried out on a Linux cluster workstation with an Intel E5-2660 CPU consisting of 8 CPU cores. The computional time taken by each model is listed in Table 3. Among them, the stress analysis model took the least time, since no failure is taken into accout. Model 1 took the longest time (over 3 days) to simulate the interaction of delamination and interface contact adjcent to the impactor. Since the upper interface damage degrades the laminate stiffness only slightly, the contact mechanism is neglected in the final model (Model 4). Without modelling the contact, Models 2 and 3 took about 15 and 20 hours, respectively. Finally, running the Model 4 took about 25 hours, which is considered acceptable.

Table 3 Computational time taken by the FE models in this study

FE model	Number of elements	Delamination definition	Computation time (h)
Stress analysis	112000 solid elements 105000 cohesive elements	No delamination	1.4
Model 1	112000 solid elements 8 surface-based cohesive contact interfaces	Interface 1-8	90.6
Model 2	112000 solid elements 22400 cohesive elements	Interface 9-22	20.5
Model 3	112000 solid elements 12800 cohesive elements	Interface 23-30	15.1
Model 4	112000 solid elements 35200 cohesive elements	Interface 9-22 and 27-30	25.1

4.2 Applicability of the efficient model in impact dynamic analysis

Model 4 is also used to simulate the structural response and damage progression of the same impact test by performing dynamic analysis. The density of IM7/977-3 laminate is 1590 kg/m^3 and the mass of the impactor is 6.8 kg. Impactor velocities of 1.71 and 2.42 m/s are applied to the model to simulate the impact energy of 10 and 20J. Dynamic analysis is carried out with the ABAQUS parallel explicit solver (v. 6.11) using the same computing facility as the quasi-static analysis. A user-defined

subroutine (VUSDFLD) is developed for implementing the 3D Hashin-type in-plane failure criterion presented in Table 2. The dynamic simulation took about 28 hours for the 10J and 20J impact; it is slighter longer than the quasi-static load analysis, but nevertheless considered being acceptable for a 32-ply quasi-isotropic laminate.

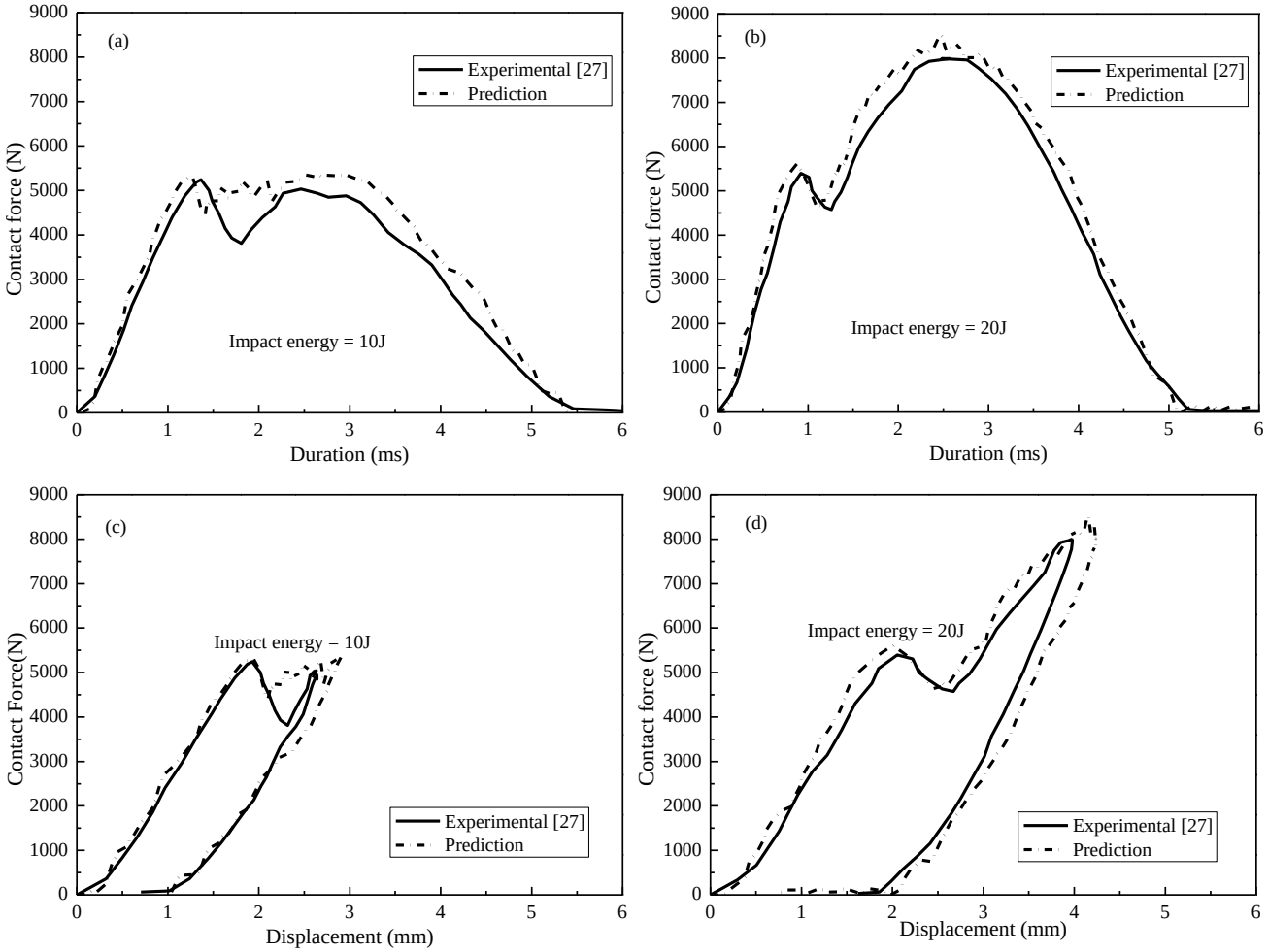

Fig. 10 Comparisons between predicted and experimental measurement of contact force vs. time (a, b) and contact force vs. displacement (c, d)

Comparisons of the predicted and experimental [27] contact force vs. time and contact force vs. displacement are shown in Fig. 10. Good agreement is achieved between the experimental and model prediction until the contact force reaches the critical impact force, i.e. the first load drop point. Beyond that, predicted contact force is higher than the experimentally measured, since only those damage modes near the mid-thickness interfaces and the back face are modelled in the new efficient FE model (Model 4). Closer delamination contours of the 10J and 20J impacts are delivered by the dynamic analysis, Figs. 11a and 11b, which are estimated by correlating the contact force to the critical force. Good agreement between the quasi-static and dynamic load analyses in terms of the delamination contour and critical force also support the strategy of modelling low-velocity impact by quasi-static load model. Beyond the critical force, the accuracy of predicted delamination area depends on the impact energy level. For the 10J impact, predicted delamination area (Fig. 11c) agrees well with the experimental result (Fig. 11e). However, for the 20J impact energy a slightly larger delamination area (Fig. 11d) is predicted by the FE model (Model 4).

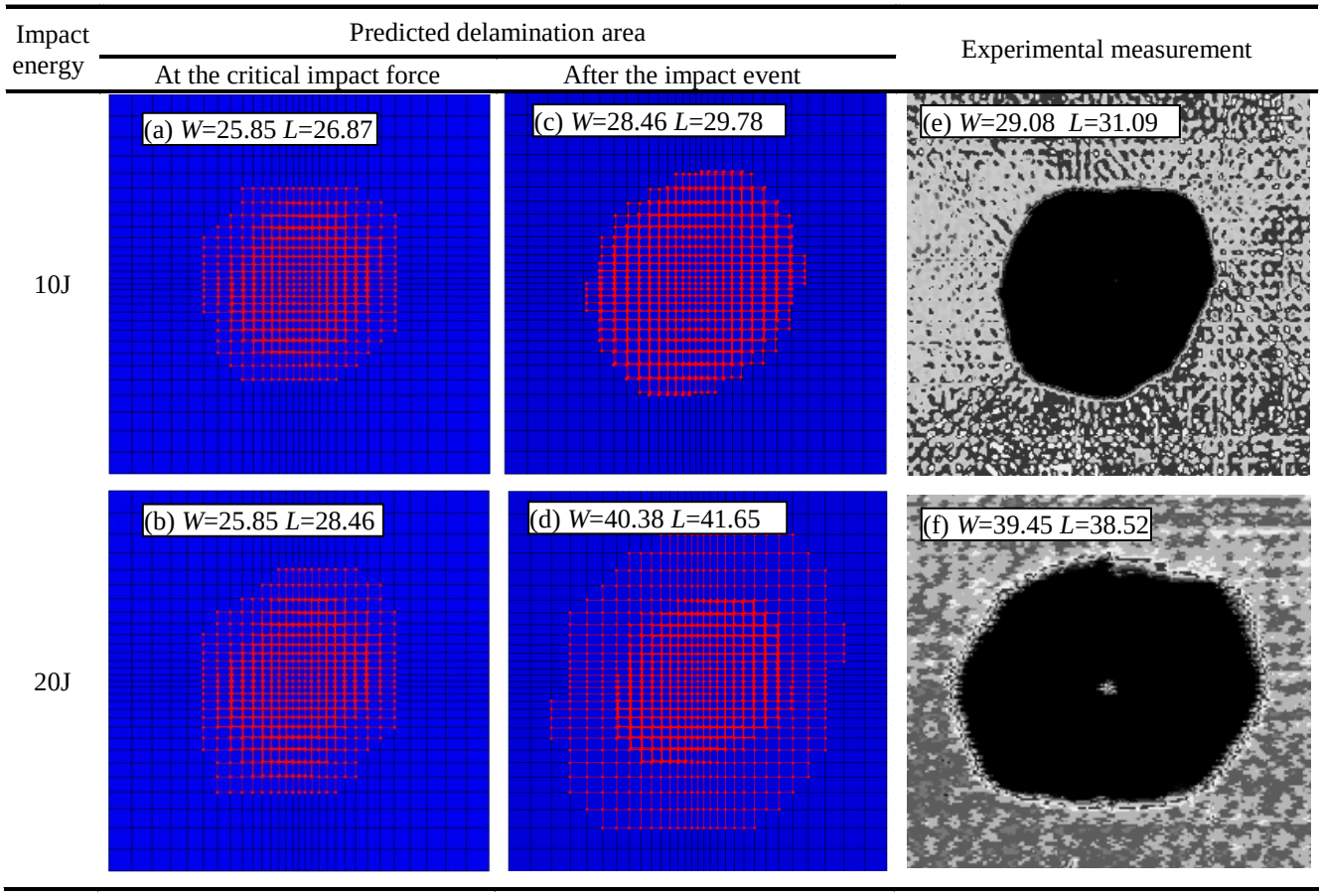

Fig. 11 Dynamic model predicted delamination areas (showing the sum of damage at different depths, unit: mm)

5. Conclusions

A computationally efficient approach is presented for predicting the critical impact force and corresponding damage of thick multi-direction composite laminates under the low velocity impact. Based on the simulation of a 4 mm thick quasi isotropic laminate, following conclusions are drawn.

(1) The stress analysis model without modelling damage provides useful information on potential failure modes and locations. According to this model, damage can occur in the upper, middle and lower interfaces.

(2) Modelling the delamination near the impact point is time consuming owing to the interaction of the interlaminar shear and compressive normal stresses; both have high values. Since the delamination onset and propagation are suppressed by the high compressive normal stress, Model 1 contribution to the laminate stiffness and critical impact force can be neglected.

(3) Both of the delamination locations, i.e. adjacent to the mid-thickness (Model 2) and next to the back face (Model 3), can cause the first load drop; the contribution depends on the material properties, laminate layup and thickness. In this study, the delamination adjacent to the mid thickness is the main causative mechanism for the first load drop of the 4 mm thick laminate.

(4) The new efficient FE model (Model 4) takes into account of the interface damage around the mid thickness and back face and gives acceptable prediction. It is computationally affordable for both quasi-static load and dynamic load analyses.

Acknowledgement

J. Zhang thanks the China Scholarship Council for supporting his visit to Cranfield University where this study was performed. J. Zhang would also thank Professor Xiaoquan Cheng at the Beihang University for helpful discussions.

References

[1] Aymerich F, Dore F, Priolo P. Prediction of impact-induced delamination in cross-ply composite laminates using cohesive interface elements. Compos Sci & Tech. 2008, 68: 2383-90

[2] Aymerich F, Dore F, Priolo P. Simulation of multiple delaminations in impacted cross-ply laminates using a finite element model based on cohesive interface elements. Compos Sci & Tech. 2009, 69:1699-1709

[3] Zhang X, Bianchi F, Liu HQ. Predicting low-velocity impact damage in composites by a quasi-static load model with cohesive interface elements. Aeronaut J. 2012, 116: 1367-81

[4] Liu HQ. Ply clustering effect on composite laminates under low-velocity impact Using FEA. MSc Thesis 2012. Cranfield University, UK

[5] Guo W, Xue P, Yang J. Nonlinear progressive damage model for composite laminates used for low-velocity impact. Appl. Math. Mech. Engl. Ed. 2013, 34, 1145-54

[6] Borg R, Nilsso L, Simonsson K. Simulation of low velocity impact on fiber laminates using a cohesive zone based delamination model. Compos Sci & Tech. 2004, 64: 279-88

[7] Feng D, Aymerich F. Finite element modelling of damage induced by low-velocity impact on composite laminates. Compos Struct. 2014,108, 161-71

[8] Bouvet C, Castanié B, Bizeul M, et al. Low velocity impact modelling in laminate composite panels with discrete interface elements. Int J Solids Struct. 2009, 46: 2809-21

[9] Riccio A, De Luca, Di Felice G, et al. Modelling the simulation of impact induced damage onset and evolution in composites. Compos B. 2014, 66: 340–47

[10] Lopes CS, Camanho PP, Gürdal Z et al. Low-velocity impact damage on dispersed stacking sequence laminates. Part II: Numerical simulations. Compos Sci & Tech. 2009, 69: 937-47

[11] González EV, Maimí P, Camanho PP et al. Effects of ply clustering in laminated composite plates under low-velocity impact loading. Compos Sci & Tech. 2011, 71: 805-17

[12] Akangah P, Shivakumar K. Assessment of impact damage resistance and tolerance of polymer nanofiber interleaved composite laminates. J of Chemical Sci & Tech. 2013, 2:39-52

[13] Feraboli P, Kedward KT. A new composite structure impact performance assessment program. Compos Sci & Tech, 2006, 66:1336–47

[14] Pérez MA, Martínez X, Oller S, et al. Impact damage prediction in carbon fiber-reinforced laminated composite using the matrix-reinforced mixing theory. Compos Struct. 2013, 104: 239-48

[15] Shyr TW, Pan YH. Impact resistance and damage characteristics of composite laminates. Compos Struct. 2003, 62: 193-203

[16] Schoeppner GA, Abrate S. Delamination threshold loads for low velocity impact on composite laminates. Compos A. 2000, 31: 903-915

[17] Olsson R, Donadon MV, Falzon BG. Delamination threshold load for dynamic impact on plates. Int J of Solids and Structures 2006, 43: 3124-41

[18] Kwon YS, Sankar BV. Indentation-flexure and low-velocity impact damage in graphite epoxy laminates. J Compos Technol Res. 1993, 15: 101-11

[19] Brindle AR, Zhang X. Predicting the compression-after-impact performance of carbon fibre composites based on impact response. Proc 17th Int Conf in Composite Materials (ICCM17), Edinburgh, UK, 27-31, July 2009

[20] Sjoblom P. Simple design approach against low velocity impact damage. Proc 32nd SAMPE Symposium, Anaheim, CA, 1987:529-39.

[21] Davies G.A.O, Robinson P. Predicting failure by debonding/delamination. AGARD: 74th Structures and Materials Meeting. 1992

[22] Davies G.A.O, Zhang X, Zhou G, Watson S. Numerical modeling of impact damage. Composites. 1994, 25:342-50.

[23] Davies, G.A.O, Zhang X. Impact damage prediction in carbon composite structures. Int Journal of Impact Engng. 1995, 16:149-70

[24] Zhang X. Impact damage in composite aircraft structures—experimental testing and numerical simulation. Proc of the Institute of Mechanical Engineers. 1998; 212:245-59.

[25] Cartié DDR, Irving PE. Effect of resin and fibre properties on impact and compression after impact performance of CFRP. Compos A. 2002, 33: 483-93

[26] Olsson R. A review of impact experiments at FFA during 1986 to 1998. The Aeronautical Research Institute of Sweden. FFA TN 1999-08, 1999.

[27] Bridlle AR. Predicting the damage tolerance of carbon fibre coupons based on impact response. 2006, MSc Thesis. Cranfield University, UK

[28] Luo GM, Lee YJ. Quasi-static simulation of constrained layered damped laminated curvature shells subjected to low-velocity impact. Compos B. 2011, 42:1233-43

[29] Sutherland LS, Guedes Soares C. The use of quasi-static testing to obtain the low-velocity impact damage resistance of marine GRP laminates. Compos B 2012, 43: 1459-67

[30] Zhang J, Zhang X. Simulating low-velocity impact induced delamination in composites by a quasi-static load model with surface-based cohesive contact, Compos Struct. 2015, 125: 51-57

[31] Tserpes KI, Labeas G, Papanikos P, et al. Strength prediction of bolted joints in graphite/ epoxy composite laminates. Compos B. 2002, 33: 521-29

[32] Abaqus analysis user's manual v. 6.11, 35.1.10. Surface-based cohesive behaviour.